

Greenhouse Gas Emissions from Wastewater Treatment Plants on a Plantwide Scale: Sensitivity and Uncertainty Analysis

Giorgio Mannina¹; Alida Cosenza²; Riccardo Gori³; Manel Garrido-Baserba⁴; Reza Sobhani⁵; and Diego Rosso⁶

Abstract: This paper presents the sensitivity and uncertainty analysis of a mathematical model for greenhouse gas emission (GHG) and energy consumption assessment in wastewater treatment plants. A sensitivity analysis was carried out (using two different methods) to determine which model factors have the greatest effect on the predicted values of the GHG production. Further, an uncertainty analysis was carried out to quantify the uncertainty of the key model outputs, such as carbon dioxide production from activated sludge treatment. The results show that influent fractionation factors, which characterize influent composition, have an important role on direct and indirect GHGs production and emission. Moreover, model factors related to the aerobic biomass growth show a relevant influence on GHGs in terms of emission from off-site power generation ($m_{\text{CO}_2\text{eq,PG}}$). Further, model factors related to the autotrophic biomass growth were found to strongly interact with other factors especially in modeling $m_{\text{CO}_2\text{eq,PG}}$. Finally, nitrous oxide (N_2O) emission associated with the effluent has the highest uncertainty, suggesting the need for a mechanistic model for N_2O production in biological treatment. DOI: 10.1061/(ASCE)EE.1943-7870.0001082. © 2016 American Society of Civil Engineers.

Author keywords: Mathematical modeling; Greenhouse gas; Energy demand; Carbon footprint; Wastewater treatment.

Introduction

Within the last decade, the interest in greenhouse gas (GHG) production and emission from wastewater treatment plants (WWTPs) has increased considerably (Monteith et al. 2005; Kampschreur et al. 2009; Ahn et al. 2010; Flores-Alsina et al. 2011; Corominas et al. 2012; Law et al. 2012). WWTPs involve three different sources of GHGs emission: direct, indirect internal, and indirect external (GRP 2008). Direct emissions from WWTPs are mainly linked to biological processes [carbon dioxide (CO_2) emission from biomass respiration; biogas fugitive emissions from anaerobic digesters, sludge processing units, and biogas lines] with physical-chemical units (e.g., pumping, grit removal, sedimentation) contributing to a minor extent (Czepiel et al. 1995). Indirect internal

emissions are associated with the consumption of imported electric or thermal energy. Finally, indirect external emissions are related to all sources not directly controlled inside the WWTP boundary (e.g., sludge disposal, production of chemicals that are used in the plant, and transportation by contractors and haulers). The main GHGs emitted from a WWTP are CO_2 , methane (CH_4), and nitrous oxide (N_2O). The fraction of short-lived carbon in the wastewater is not of concern for CO_2 emission; however, attention must be given to long-lived carbon and the other GHGs (Law et al. 2013). Among the GHGs emitted from WWTPs, N_2O merits investigation and should be reduced due to its high global warming potential (GWP) that is approximately 298 times higher than CO_2 GWP (IPCC 2006). Therefore, even low amounts of N_2O emission are undesirable and raise concern. Moreover, although current attention is focused on the N_2O emission, the CH_4 fugitive emission remains an open question, and to date there is no survey or study available with limited uncertainty (IPCC 2006).

A quantification of GHGs, regardless of their origin, is necessary to improve the understanding of carbon flows within treatment and the sustainability of WWTPs (Caniani et al. 2015). Furthermore, the estimation of GHGs should be considered during the design, operation, and optimization of treatment processes (Flores-Alsina et al. 2011). Several recent attempts have been made to better understand GHG production (Foley et al. 2010; Daelman et al. 2012), to quantify and measure GHG emission (LGO 2008; GWRC 2011; Townsend-Small et al. 2011), and to predict and control their production (Flores-Alsina et al. 2011; Corominas et al. 2012; Ni et al. 2013b, a). However, literature shows that knowledge of the dynamics and magnitude of N_2O production and emission is still poor and that further investigation is needed (Ni et al. 2013b). With regard to GHG quantification and measuring techniques, literature shows a wide range of measured GHG emissions (inter alia, Czepiel et al. 1995; IPCC 2006; Ahn et al. 2010; GWRC 2011; Daelman et al. 2012). This wide range reveals the need to improve

¹Associate Professor, Dipartimento di Ingegneria Civile, Ambientale, Aerospaziale, dei Materiali, Università degli Studi di Palermo, Viale delle Scienze, 90128 Palermo, Italy (corresponding author). E-mail: giorgio.mannina@unipa.it

²Postdoctoral Fellow, Dipartimento di Ingegneria Civile, Ambientale, Aerospaziale, dei Materiali, Università degli Studi di Palermo, Viale delle Scienze, 90128 Palermo, Italy. E-mail: alida.cosenza@unipa.it

³Assistant Professor, Dept. of Civil and Environmental Engineering (DICEA), Univ. of Florence, Via Santa Marta 3, 50139 Florence, Italy. E-mail: riccardo.gori@dicea.unifi.it

⁴Postdoctoral Fellow, Dept. of Civil and Environmental Engineering, Univ. of California, Irvine, CA 92697-2175. E-mail: mgbaserba@gmail.com

⁵Postdoctoral Fellow, Dept. of Civil and Environmental Engineering, Univ. of California, Irvine, CA 92697-2175. E-mail: rsobhani@uci.edu

⁶Associate Professor, Dept. of Civil and Environmental Engineering, Univ. of California, Irvine, CA 92697-2175. E-mail: rossodr@gmail.com

Note. This manuscript was submitted on January 14, 2015; approved on October 28, 2015; published online on January 27, 2016. Discussion period open until June 27, 2016; separate discussions must be submitted for individual papers. This paper is part of the *Journal of Environmental Engineering*, © ASCE, ISSN 0733-9372.

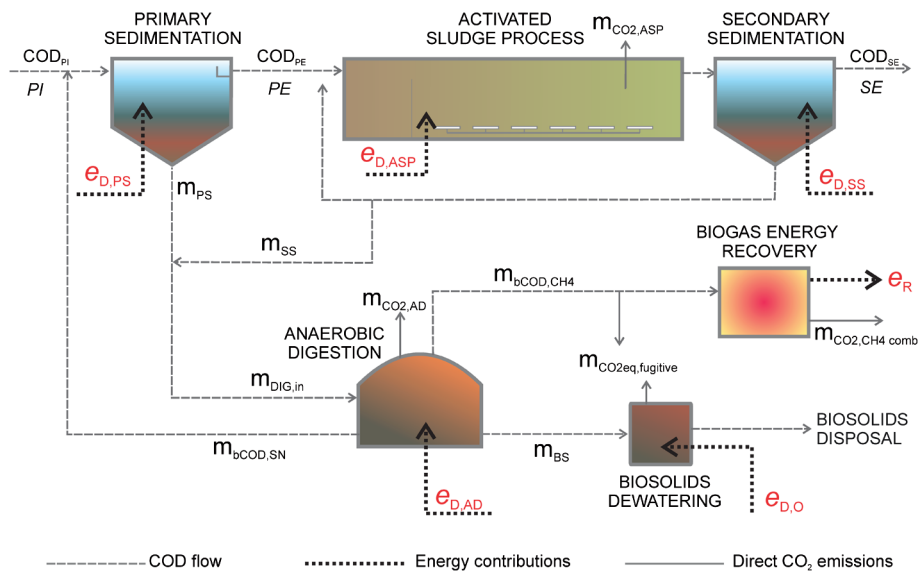


Fig. 1. Wastewater treatment plants layout and depiction of chemical oxygen demand and energy flows

the understanding of process dynamics as well as the measurement techniques and tools for GHG quantification.

Mathematical models may allow for the identification of key processes and operational conditions that merit further investigation or modification in order to reduce GHG emission. Different types of mathematical models (i.e., empirical, mechanistic, or simple comprehensive process models) are available for estimating GHG emission (e.g., Monteith et al. 2005; Hiatt and Grady 2008; Rosso and Stenstrom 2008; Foley et al. 2010; Flores-Alsina et al. 2011; Gori et al. 2011; Ni et al. 2011; Mannina and Cosenza 2015). All of these models have provided a valuable contribution to the understanding of how to reduce the GHG emission from WWTPs. Plantwide mathematical models may help the understanding of the effect of operational parameters on GHG emission and can be used to develop strategies aimed at reducing GHG emission and improving environmental protection (Flores-Alsina et al. 2014). In fact, a plantwide modeling approach that includes GHG emission as state variables enhances the overall sustainability of the process control or operational strategies (Flores-Alsina et al. 2014). However, despite the useful insights derived from mathematical models of GHG emission from WWTPs, the results are likely to be subjected to a high degree of uncertainty (Sweetapple et al. 2013). The assessment of the most relevant sources of uncertainty in GHG emission modeling can be useful for improving the model prediction. In this context, both sensitivity and uncertainty analyses can be useful tools for identifying the key sources that control model outputs (Pagilla et al. 2009). Specifically, the use of global sensitivity analysis (GSA), which gives information on the interaction among model factors, should be preferred. Despite such potentialities, only a few studies have been carried out estimating uncertainty and sensitivity of GHG models, mainly focusing on complex mechanistic ones (among others, Sweetapple et al. 2013).

As far as the authors are aware, modelers dealing with simple comprehensive process models for GHG assessment often do not apply sensitivity and uncertainty analysis as a common practice. Such an aspect would allow assessment of the robustness of the results versus model assumptions. Further, the model results, especially for the case of simple comprehensive process models, could be further improved by means of sensitivity and uncertainty analysis. Indeed, by selecting important, noninfluential, or interacting

model factors, the modeler will be able to determine the model factors on which the attention should be focused on.

This paper is aimed at pinning down the key sources of uncertainty in modeling the GHG emissions and energy requirement from WWTPs. Further, the study has the additional goal of demonstrating the importance in the estimation of the sensitivity and uncertainty for getting robust model results.

To accomplish such an aim, a plantwide simple comprehensive process model for carbon and energy footprint of WWTPs was adopted. Further, sensitivity and uncertainty analyses were performed to better understand the role of each model factor in influencing GHG production. *Factors* is a term widely used in the sensitivity analysis literature and includes model parameters and model input variables (Saltelli et al. 2008). The results make it possible to specify which model factors have a dominant role (also in terms of interactions) in key model outputs, and thus deserve to be accurately evaluated for model calibration and application.

Materials and Methods

Plant and Mathematical Model Description

The model used for the analysis employed in this study was developed for modeling the carbon and energy footprint of a conventional activated sludge WWTP based on a modified Ludzack-Ettinger process for denitrification, with primary sedimentation, anaerobic stabilization of the sludge, and energy recovery from biogas (Gori et al. 2011, 2013). Fig. 1 depicts a model layout. The model evaluates the total equivalent CO_2 ($\text{CO}_{2,\text{eq}}$) emission ($\text{kg}_{\text{CO}_{2,\text{eq}}}/\text{day}$ or $\text{g}_{\text{CO}_{2,\text{eq}}}/\text{treated volume}$) as the sum of direct CO_2 emission from biological processes [activated sludge process (ASP) and anaerobic digestion (AD)] ($m_{\text{CO}_{2,\text{ASP}}} + m_{\text{CO}_{2,\text{AD}}}$), direct CO_2 emission from biogas combustion ($m_{\text{CO}_{2,\text{CH}_4,\text{comb}}}$), indirect CO_2 emission from biogas combustion ($m_{\text{CO}_{2,\text{eq},\text{CH}_4,\text{comb}}}$), indirect CO_2 emission from off-site power generation ($m_{\text{CO}_{2,\text{eq},\text{PG}}}$), $\text{CO}_{2,\text{eq}}$ offset from biogas energy recovery ($m_{\text{CO}_{2,\text{eq},\text{offset}}}$), and $\text{CO}_{2,\text{eq}}$ emission due to CH_4 fugitive emission ($m_{\text{CO}_{2,\text{eq},\text{fugitive}}}$). In contrast to the previous version (i.e., Gori et al. 2011), the model calculates the contribution of $\text{CO}_{2,\text{eq}}$ due to the N_2O discharge ($m_{\text{N}_2\text{O},\text{eff}}$) with the effluent ($m_{\text{CO}_{2,\text{eq},\text{N}_2\text{O},\text{eff}}}$) and to the total biosolids (TB) discharge ($m_{\text{CO}_{2,\text{eq},\text{TB}}}$) as in the following:

$$m_{\text{CO}_2\text{eq}} = m_{\text{CO}_2\text{,ASP}} + m_{\text{CO}_2\text{,AD}} + m_{\text{CO}_2\text{,CH}_4\text{comb}} + m_{\text{CO}_2\text{eq,CH}_4\text{comb}} + m_{\text{CO}_2\text{eq,PG}} - m_{\text{CO}_2\text{eq,offset}} + m_{\text{CO}_2\text{eq,fugitive}} + m_{\text{CO}_2\text{eq,N}_2\text{O,eff}} + m_{\text{CO}_2\text{eq,TB}} \quad (1)$$

where $m_{\text{CO}_2\text{eq,fugitive}}$ contains the $\text{CO}_2\text{,eq}$ emission due to CH_4 fugitive emission ($m_{\text{CO}_2\text{eq,CH}_4\text{,fugitive}}$) and due to CH_4 released during biosolids dewatering ($m_{\text{CO}_2\text{eq,CH}_4\text{,dewatering}}$). Regarding the energy demand (e_D , kJ/day), the model estimates the contributions from primary sedimentation ($e_{D,PS}$), activated sludge process aeration ($e_{D,ASP}$), secondary sedimentation ($e_{D,SS}$), anaerobic digestion ($e_{D,AD}$), and other equipment ($e_{D,O}$) by means of the following equation:

$$e_D = e_{D,PS} + e_{D,ASP} + e_{D,SS} + e_{D,AD} + e_{D,O} \quad (2)$$

The energy recovery (e_R , kJ/day) is calculated from the biogas (BG) production (m_{BG} , kg/day) multiplied by the efficiency of the energy unit recovery (ER) η_{ER} (-) and the caloric value of the biogas h_{BG} (kJ/kg $_{BG}$):

$$e_R = \eta_{ER} h_{BG} m_{BG} \quad (3)$$

The model was applied to a municipal water reclamation plant ($Q \sim 60,000 \text{ m}^3 \text{ day}^{-1}$) located in the United States in a warm area

($T_{\text{ww,avg}} = 20^\circ\text{C}$) with process schematic matching that of Fig. 1, with the addition of head works and disinfection. The WWTP influent is characterized by [average \pm standard deviation (SD)]: chemical oxygen demand (COD) $541 \pm 100 \text{ mg/L}$, biochemical oxygen demand (BOD_5) $243 \pm 48 \text{ mg/L}$, total suspended solids (TSS) $308 \pm 56 \text{ mg/L}$, volatile suspended solids (VSS) $263 \pm 50 \text{ mg/L}$, and ammonia ($\text{NH}_4\text{-N}$) $28.8 \pm 3.8 \text{ mg/L}$. The WWTP is operated with an average mean cell residence time of 8.5 days.

For further details, refer to Gori et al. (2011, 2013). Table 1 summarizes the symbol, description, unit, default value at 20°C , variation range, and literature references of each of the model factors. Specifically, Table 1 summarizes emission factors (EFs) and stoichiometric, kinetic, conversion, and fractionation factors. These latter factors characterize the wastewater composition with respect to the total COD. Table 2 summarizes the model outputs.

Sensitivity Analysis Methods

In order to gain insights in the evaluation of GHG at plantwide scale, two GSA methods have been applied: standardized regression coefficient (SRC) and extended Fourier amplitude sensitivity test (Extended-FAST). The application of the Extended-FAST

Table 1. Summary of Symbols, Units, Range, and Literature References for Each Model Factor

Symbol	Description	Unit	Default ($T = 20^\circ\text{C}$)	Minimum	Maximum	Reference
μ	Maximum growth rate of heterotrophic biomass	day^{-1}	5.9850	4.0000	8.0000	Hauduc et al. (2011)
k_s	Half-saturation parameter for heterotrophic biomass	gCOD m^{-3}	19.9500	19.0000	21.0000	Hauduc et al. (2011)
k_d	Decay rate for heterotrophic biomass	day^{-1}	0.1197	0.0500	1.6000	Hauduc et al. (2011)
Y_H	Yield for heterotrophic biomass growth	gVSS gCOD^{-1}	0.3990	0.3800	0.7500	Hauduc et al. (2011)
μ_N	Maximum growth rate of autotrophic biomass	day^{-1}	0.4988	0.2000	1.2000	Hauduc et al. (2011)
K_N	Half-saturation parameter for autotrophic biomass	$\text{gNH}_4\text{-N m}^{-3}$	0.4988	0.5000	1.5000	Hauduc et al. (2011)
k_{dN}	Decay rate for autotrophic biomass	day^{-1}	0.1197	0.0400	0.1605	Hauduc et al. (2011)
Y_N	Yield of autotrophic biomass growth	$\text{gVSS gNH}_4\text{-N}$	0.1197	0.1200	0.2520	Brun et al. (2002)
$k_{d,\text{dig}}$	Decay rate for biomass during digestion	day^{-1}	0.0299	0.0150	0.0300	Cakir and Stenstrom (2005)
$Y_{H,\text{dig}}$	Yield for heterotrophic biomass growth during digestion	gVSS gCOD	0.0798	0.0400	0.0800	Cakir and Stenstrom (2005)
pCOD/VSS	Ratio between particulate COD and volatile suspended solids	—	1.4663	1.0700	1.8700	Gori et al. (2011)
nbsCOD _{IN}	Fraction of soluble nonbiodegradable COD in influent wastewater	—	0.0339	0.0340	0.1200	Mannina et al. (2011), Gori et al. (2011)
pbCOD _{IN}	Fraction of particulate biodegradable COD in influent wastewater	—	0.4479	0.1000	0.4500	Mannina et al. (2011), Gori et al. (2011)
npbCOD _{IN}	Fraction of particulate nonbiodegradable COD in influent wastewater	—	0.2454	0.0500	0.2500	Mannina et al. (2011), Gori et al. (2011)
bsCOD _{IN}	Fraction of soluble biodegradable COD in influent wastewater	—	0.2728	—	—	—
nbsCOD _{PI}	Fraction of soluble nonbiodegradable COD in the primary effluent	—	0.0698	0.0340	0.1200	Mannina et al. (2011), Gori et al. (2011)
pbCOD _{PI}	Fraction of particulate biodegradable COD in the primary effluent	—	0.3082	0.1000	0.4500	Mannina et al. (2011), Gori et al. (2011)
npbCOD _{PI}	Fraction of particulate nonbiodegradable COD in the primary effluent	—	0.1357	0.0500	0.2500	Mannina et al. (2011), Gori et al. (2011)
bsCOD _{PI}	Fraction of soluble biodegradable COD in the primary effluent	—	0.4863	—	—	—
Q _{dewa}	Fraction of the influent flow that achieves the dewatering section	—	0.0100	0.0090	0.0110	Gori et al. (2011)
EF _{N2O}	N ₂ O emission factor due to the effluent	$\text{gCO}_2\text{eq L}^{-1}$	0.0038	0.0038	0.0780	IPCC (2006)
EF _{CO2}	CO ₂ emission factor due to the headworks	$\text{gCO}_2 \text{L}^{-1}$	0.0045	0.0041	0.0050	Czepllel et al. (1993)
EF _{CH4}	CH ₄ emission factor due to the headworks	$\text{gCO}_2\text{eq L}^{-1}$	0.0001	0.0001	0.0002	Czepllel et al. (1993)
INVSS _{PS}	N content of biomass in the primary sludge	kgN kgVSS^{-1}	0.0858	0.0665	0.1200	Brun et al. (2002), Gori et al. (2011)
INVSS _{SS}	N content of biomass in the secondary sludge	kgN kgVSS^{-1}	0.1197	0.0665	0.1200	Brun et al. (2002), Gori et al. (2011)
iCOD _{NOx}	Conversion factor for NO _x in COD	$\text{kgO}_2\text{kgN}^{-1}$	4.3192	3.8970	4.7630	Gori et al. (2011)
iCOD _{N2}	Conversion factor for N ₂ in COD	$\text{kgO}_2\text{kgN}^{-1}$	2.8529	2.5740	3.1460	Gori et al. (2011)
CH _{4-SE}	CH ₄ specific energy	MJ m^{-3}	35.7105	32.2200	39.3800	Gori et al. (2011)

Table 2. Symbol and Description of Each Model Output

Symbol	Description
$m_{CO_2,ASP}$	CO ₂ emission due to biomass respiration
$m_{CO_2,CH_4,comb}$	CO ₂ emission due to biogas combustion
$m_{CO_2eq,CH_4,comb}$	Equivalent CO ₂ due to CH ₄ emission during biogas combustion
$m_{CO_2eq,CH_4,fugitive}$	Equivalent CO ₂ due to fugitive CH ₄ emission
$m_{CO_2eq,CH_4,dewatering}$	Equivalent CO ₂ due to CH ₄ emission in the dewatering unit
$m_{CO_2eq,N_2O,eff}$	Equivalent CO ₂ due to N ₂ O emission with the effluent discharge
$m_{CO_2eq,PG}$	Equivalent CO ₂ emission due to plant power requirements
$m_{CO_2eq,offset}$	Equivalent CO ₂ emission credit due to energy recovery
$m_{CO_2eq,TB}$	Equivalent CO ₂ emission related to total biosolids discharge
η_{CODPS}	COD removal efficiency of the primary settler

method is aimed at quantifying model factor interactions. In the following, a brief description of each GSA method applied here will be presented.

SRC Method

The SRC method consists of running a Monte Carlo (MC) simulation by using a randomly sampled factor matrix. A multivariate linear regression is then performed between the model output (y) and the factors (x_i) (Saltelli et al. 2008) [Eq. (4)]

$$y = b_0 + \sum_{i=1}^n b_i \cdot x_i + \varepsilon \quad (4)$$

where n = number of factors; b_i = regression slopes; and ε = random error of the regression model.

The SRCs are the standardised regression slopes [Eq. (5)]

$$SRC(x_i) = \beta_i = b_i \cdot \sigma_{x_i} / \sigma_y \quad (5)$$

where β_i = regression slope; and σ_{x_i} and σ_y = factor and model output standard deviation, respectively. β_i is a valid measure of sensitivity if the coefficient of determination (R^2), which indicates the portion of total variance explained by the regression model, is higher than 0.7 (Saltelli et al. 2008). The sign of β_i indicates its positive (sign +) or negative (sign -) effect (Saltelli et al. 2008). A high absolute value of β_i indicates a relevant effect of the related i th factor on the model output. In case of linear models $\sum \beta_i^2 = 1$, otherwise this sum, which represents the model coefficient of determination R^2 , is lower than 1 (Saltelli et al. 2008).

The SRC method does not provide information about the interaction among factors. Therefore, by adopting the SRC method the important (factors prioritization) and noninfluential (factors fixing) factors may be correctly distinguished only in case of linear models.

Typical numbers of MC simulations found in literature are between 500 and 1,000 (Cosenza et al. 2013b; Neumann 2012).

Variance-Based Method

Variance-based methods are based on the variance decomposition theorem and provide a measure of sensitivity for every relationship between the model output and model factors: nonlinear, nonmonotonic, or nonadditive (Neumann 2012).

The Extended-FAST method, as proposed by Saltelli et al. (2008), provides two sensitivity indexes for each model factor:

the first-order effect index (S_i) and the total-effect index (S_{Ti}). S_i measures how the i th factor contributes to the variance of the model output [$\text{var}(Y)$] without taking into account the interactions with other factors; it is expressed as

$$S_i = \frac{\text{var}_{x_i}[E_{x_{-i}}(Y|x_i)]}{\text{var}(Y)} \quad (6)$$

where E = expectancy operator; Y = model output; and var = variance. The subscripts indicate that the operation is either applied over the i th factor X_i or over all model factors except the i th model factor X_{-i} (Saltelli et al. 2008).

S_{Ti} is expressed as

$$S_{Ti} = 1 - \frac{\text{var}_{x_{-i}}[E_{x_i}(Y|x_{-i})]}{\text{var}(Y)} \quad (7)$$

The difference between S_{Ti} and S_i represents the interaction among the model factors.

In the context of factor fixing, the analysis of S_{Ti} has to be performed. If the S_i value is small, it does not necessarily mean that the factor may be fixed anywhere within its range because a high S_{Ti} value would indicate that the factor is involved in interactions.

The Extended-FAST method requires $n \times NR$ simulations, where n is the number of factors and NR is the number of repetition of MC simulations per factor within its range [NR = 500 to 1,000 according to Saltelli et al. (2008), Neumann (2012), Cosenza et al. (2013b), and Mannina et al. (2014)].

GSA Results Analysis

The results of the two GSA methods have been compared in terms of similarity and differences of classification into important and noninfluential factors. This comparison has been conducted by analyzing the Venn diagram of the results. This diagram will be developed by drawing circles containing the results of each GSA method, and the overlapping area or intersection among the circles contains the same results. It must be stressed that such a comparison helps identify the model factors that contribute significantly to GHG emissions for wastewater treatment.

Uncertainty Analysis

The uncertainty analysis has been performed by running the MC simulations; results of the uncertainty analysis for each variable have been interpreted by analyzing the cumulative distribution function (CDF).

Simulation Conditions and Numerical Settings

Sensitivity analysis has been performed by considering 26 model factors (Table 1) and 10 model outputs (Table 2). Variables $bsCOD_{IN}$ and $bsCOD_{PI}$ were indirectly varied in the random sampling procedure for the sensitivity analysis. Indeed, $bsCOD_{IN}$ and $bsCOD_{PI}$ represent the complement of the fractionation factors related to the influent and the effluent, respectively.

Due to the lack of knowledge about the distribution of the model factors, each of the two GSA methods was applied considering a uniform distribution for all factors (Freni and Mannina 2010). The widest variation range found in literature has been used for each model factor (Cosenza et al. 2013a). The two GSA methods were applied using the sensitivity package developed in the R environment (Pujol 2007).

To classify important, noninfluential, and interacting factors, the thresholds of the sensitivity measures were selected.

The thresholds for the assessment of the important factors were chosen according to previous studies (Sin et al. 2011; Cosenza et al. 2013b; Neumann 2012; Mannina et al. 2014). More specifically, the threshold value of 0.1 was employed for the absolute value of β_i . All factors having the absolute value of β_i higher than 0.1, at least for one model output, were considered important for the SRC application. For the S_i a threshold of 0.01 was selected, and this choice was related to the fact that for a linear model $S_i = \beta_i^2$ (Cosenza et al. 2013b; Neumann 2012; Mannina et al. 2014). Factors with a S_i value greater than 0.01, at least for one model output, were classified as important. Interacting model factors were selected using the normalized index value (S_{Ni}), which corresponds to the ratio between the interaction of the i th model factor related to one model output and the maximum value among the interactions for that model output (Cosenza et al. 2013b; Mannina et al. 2014). By considering S_{Ni} , it is possible to fix the same threshold for all model outputs and at least one factor will be classified as a factor with high interaction for each model output (Weijers and Vanrolleghem 1997; Cosenza et al. 2013b; Mannina et al. 2014). Factors with S_{Ni} greater than 0.5 for at least one model output were considered to be interacting. Model factors with S_{Ni} and S_i values lower than 0.5 and 0.01, respectively, were considered to be noninfluential.

The uncertainty analysis was performed by considering the results of GSA applications. In particular, uncertainty analysis has been performed after applying each method and considering only the important model factors and fixing the noninfluential factors.

Results and Discussion

Sensitivity Analysis

The SRC method has been applied by running 600 model simulations and generating a model factor matrix having 600×26 dimension. These model simulation runs have been derived verifying the convergence of the sensitivity analysis method (Cosenza et al. 2013b; Vanrolleghem et al. 2015). Results show that the SRC method is applied within the applicability range ($R^2 > 0.7$) suggested in literature, indicating that the β_i is a valid measure of sensitivity (Table 3). Indeed, for each model output, the R^2 value is almost always greater than 0.9. Furthermore, the model can be considered linear to select important and noninfluential model factors by means of the β_i value. Indeed, even though the SRC method does not provide information about the interaction among factors, the high degree of linearity of the model enables adoption of the value of β_i to distinguish important (factor prioritization) and noninfluential factors (factor fixing). The lowest value of R^2 (0.89) has been obtained for the model output $m_{CO2eq,PG}$, and this result is likely due to the higher interaction among factors for this model output (Table 3).

The Extended-FAST method has been applied by running 26,000 model simulations and generating a model factor matrix with $NR = 1,000$. The sum of S_i explains more than 90% of the total variance for all model outputs except for the $m_{CO2eq,PG}$ (Table 3). These results indicate that the model is linear and additive. This statement is also confirmed by the value of the sum of S_{Ti} , which is always close to 1 except for the $m_{CO2eq,PG}$ model output. Indeed, results related to the $m_{CO2eq,PG}$ show that for this model output a quite high degree of interaction among factors takes place

Table 3. Symbol and Important Model Factors Selected on the Basis of β_i for Each Model Output

Factors	$m_{CO2,ASP}$	$m_{CO2,CH4,comb}$	$m_{CO2eq,CH4,comb}$	$m_{CO2eq,CH4,fugitive}$	$m_{CO2eq,CH4,dewatering}$	$m_{CO2eq,N2O,eff}$	$m_{CO2eq,PG}$	$m_{CO2eq,offset}$	$m_{CO2eq,TB}$	η_{CODPS}
	β_i	β_i	β_i	β_i	β_i	β_i	β_i	β_i	β_i	β_i
μ	-0.001	0.013	0.013	0.013	0.000	0.000	0.006	0.009	-0.008	0.000
k_s	0.003	-0.018	-0.018	-0.018	0.000	0.000	0.008	-0.011	0.006	0.000
k_d	0.405	-0.317	-0.317	-0.317	0.000	0.000	0.321	-0.312	-0.146	0.000
Y_H	-0.008	0.085	0.085	0.085	0.000	0.000	-0.246	0.081	0.229	0.000
μ_N	0.006	0.023	0.023	0.023	0.000	0.000	0.020	0.019	-0.015	0.000
K_N	0.001	-0.006	-0.006	-0.006	0.000	0.000	-0.003	-0.004	-0.005	0.000
k_{dN}	0.016	-0.033	-0.033	-0.033	0.000	0.000	0.018	-0.036	-0.014	0.000
Y_N	-0.018	0.014	0.014	0.014	0.000	0.000	-0.046	0.011	0.018	0.000
$k_{d,dig}$	-0.019	0.036	0.036	0.036	0.000	0.000	-0.003	0.032	-0.005	0.000
$Y_{H,dig}$	-0.011	-0.023	-0.023	-0.023	0.000	0.000	-0.007	-0.022	-0.012	0.000
$pCOD/VSS$	-0.001	0.380	0.380	0.380	0.000	0.000	0.072	0.373	0.014	0.000
$nbsCOD_{IN}$	-0.226	-0.033	-0.033	-0.033	0.000	0.000	-0.217	-0.031	-0.049	0.000
$pbCOD_{IN}$	-0.642	0.451	0.451	0.451	0.000	0.000	-0.502	0.446	-0.739	0.890
$npbCOD_{IN}$	-0.567	-0.572	-0.572	-0.572	0.000	0.000	-0.614	-0.562	0.532	0.508
$nbsCOD_{PI}$	0.008	-0.005	-0.005	-0.005	0.000	0.000	0.021	-0.007	-0.003	0.000
$pbCOD_{PI}$	0.010	-0.176	-0.176	-0.176	0.000	0.000	-0.068	-0.173	-0.031	0.000
$npbCOD_{PI}$	-0.008	0.175	0.175	0.175	0.000	0.000	0.045	0.166	0.035	0.000
Q_{dewa}	0.009	-0.011	-0.011	-0.011	0.798	0.000	0.036	-0.016	0.001	0.000
EF_{N2O}	0.002	0.012	0.012	0.012	0.000	1.000	-0.007	0.014	0.010	0.000
EF_{CO2}	0.031	-0.028	-0.028	-0.028	0.000	0.000	0.020	-0.028	0.001	0.000
EF_{CH4}	0.019	-0.009	-0.009	-0.009	0.576	0.000	0.017	-0.008	-0.007	0.000
$iNVSS_{PS}$	0.000	-0.023	-0.023	-0.023	0.000	0.000	0.020	-0.023	0.000	0.000
$iNVSS_{SS}$	0.006	0.005	0.005	0.005	0.000	0.000	-0.024	0.004	-0.019	0.000
$iCOD_{NOx}$	-0.012	0.005	0.005	0.005	0.000	0.000	0.179	0.006	0.002	0.000
$iCOD_{N2}$	0.010	-0.002	-0.002	-0.002	0.000	0.000	-0.120	-0.003	-0.006	0.000
$CH_{4,SE}$	0.006	0.002	0.002	0.002	0.000	0.000	-0.014	0.174	0.000	0.000
R^2	0.920	0.900	0.900	0.900	0.999	0.999	0.890	0.900	0.960	0.999
$\Sigma\beta_i^2$	0.952	0.851	0.851	0.851	0.968	1.000	0.905	0.852	0.909	1.051

Note: Important model factors are in bold.

(sum of $S_{Ti} = 4.761$) (Table 3). Except for $m_{CO_2eq,PG}$ and η_{CODPS} , all important model factors are interacting with each other. Hence, the high degree of linearity flattens the selection of interacting factors for the greater part of the model outputs analyzed.

For the sake of conciseness, only the results related to $m_{CO_2,ASP}$, $m_{CO_2eq,CH_4,comb}$, $m_{CO_2eq,CH_4,dewatering}$, and $m_{CO_2eq,PG}$ will be discussed in detail (Fig. 2). These model outputs have been selected because they are the most representative of the major processes occurring inside the modeled system.

By analyzing Fig. 2, one may observe that four factors have significant impact on $m_{CO_2,ASP}$ [Fig. 2(a), Tables 3 and 4], both for SRC and Extended-FAST application. Specifically, k_d , $nbsCOD_{IN}$, $pbCOD_{IN}$, and $npbCOD_{IN}$ have for $m_{CO_2,ASP}$ the absolute value of β_i and the value of S_i higher than 0.1 and 0.01, respectively. Moreover, factor k_d is also interacting with having the S_{Ni} value equal to 1. Among these four factors, three ($nbsCOD_{IN}$, $pbCOD_{IN}$, and $npbCOD_{IN}$) are related to the influent wastewater COD fractionation and one (k_d) is related to the heterotrophic biomass kinetics. The effect of influent COD fractionation is certainly the most interesting from a process point of view. In fact, the influent fractionation factors influence the bCOD available for biomass growth and consequently the $m_{CO_2,ASP}$ value. For example, the higher the $nbsCOD_{IN}$ fraction, the lower the availability of

substrate to be degraded during the biomass metabolism. Hence, $m_{CO_2,ASP}$ is reduced as a result of the conservative nature of $nbsCOD_{IN}$. The factor k_d represents the specific decay rate of heterotrophic biomass and significantly influences $m_{CO_2,ASP}$ because it regulates the endogenous decay of heterotrophic biomass. The higher is k_d , the higher is the $m_{CO_2,ASP}$ as underlined by the positive value of β_i .

For $m_{CO_2eq,CH_4,comb}$ [Fig. 2(b), Tables 3 and 4], k_d , $pCOD/VSS$, $pbCOD_{IN}$, $npbCOD_{IN}$, $pbCOD_{PI}$, and $npbCOD_{PI}$ appear to have the most significant impacts on the basis of both β_i and S_i . Furthermore, all of these, except $pbCOD_{PI}$ and $npbCOD_{PI}$, are also interacting. The interaction of these two latter model factors is likely due to the fact that the amount of COD removal in the primary settler is strongly related to the COD influent fractionation factors (e.g., $pbCOD_{IN}$ and $npbCOD_{IN}$).

Among these factors, the most relevant for process diagnostics are $pCOD/VSS$, $pbCOD_{IN}$, and $npbCOD_{IN}$. The fraction of $pCOD$ or $npbCOD$ strongly influences the amount of CH_4 produced during anaerobic digestion due to the different nature of the bCOD removed in the primary settler. In fact, higher particulate in the influent wastewater entails higher bCOD removal in the primary settler, whose sludge is typically higher in COD per unit VSS mass removed than secondary sludge (Gori et al. 2011). This circumstance leads to an increase of the CH_4 production in the anaerobic tank and consequently of the equivalent CO_2 emitted during the combustion of CH_4 (Gori et al. 2013).

Two factors have a significant impact on $m_{CO_2eq,CH_4,dewatering}$, both in terms of β_i and S_i value [Fig. 2(c), Tables 3 and 4], namely Q_{dewa} and EF_{CH_4} . Indeed, these factors represent, respectively, the percentage of flow (with respect to the influent wastewater flow) that reaches the dewatering section and the emission factor of CH_4 from the dewatering. These two model factors have a positive influence on $m_{CO_2eq,CH_4,dewatering}$ as underlined by their positive sign of β_i . Such a result shows that a linear relationship exists among the $m_{CO_2eq,CH_4,dewatering}$, Q_{dewa} , and EF_{CH_4} . This statement can be corroborated by the value of R^2 (for SRC application) and the sum of S_i and sum of S_{Ti} (for Extended-FAST application), which are very close to 1.

For the $m_{CO_2eq,PG}$ model output, seven factors proved to be important in terms of both β_i and S_i value: k_d , Y_H , $nbsCOD_{IN}$, $pbCOD_{IN}$, $npbCOD_{IN}$, $iCOD_{NOx}$, and $iCOD_{N_2}$. Among these factors, the first two are directly related to the kinetic and stoichiometric characteristics of heterotrophic biomass. Thus, because the WWTP energy demand is mainly due to the activated sludge processes (WEF 2009), the influence of k_d and Y_H on the $m_{CO_2eq,PG}$ model output is associated with their influence on regulating the heterotrophic active biomass in the aerobic tank and consequently on the aeration energy requirements. A comment can be made on the relationships among temperature, biokinetics, and carbon footprint: as global temperature rises, the wastewater temperature rises, and hence so does the value of k_d . Because k_d has a nonlinear response with temperature increase (it increases by nearly an order of magnitude between 10 and 30°C), and because in the same temperature range the bacterial efficiency in removing bCOD from the influent changes by a small adjustment, the consequence is that increasing temperatures should result in CO_2 emission from endogenous respiration (driven by k_d) that is higher in proportion than the CO_2 emission from aerobic respiration, in essence a positive feedback mechanism for CO_2 emission. The influence of $nbsCOD_{IN}$, $pbCOD_{IN}$, and $npbCOD_{IN}$ is mainly due to the ability of these factors to regulate the availability of soluble COD required for the biological processes. For example, as the fraction of sCOD decreases, the oxygen required for the aerobic processes decreases,

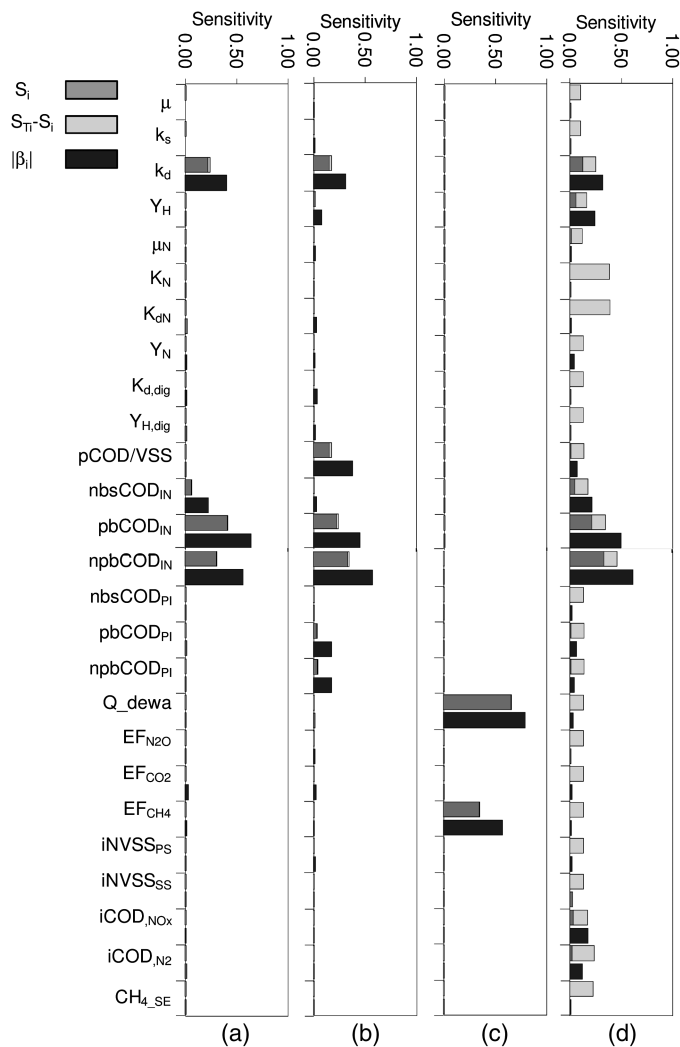


Fig. 2. Sensitivity ($|\beta_i|$, S_i , and S_{Ti}) of all factors for (a) $m_{CO_2,ASP}$; (b) $m_{CO_2eq,CH_4,comb}$; (c) $m_{CO_2eq,CH_4,dewatering}$; (d) $m_{CO_2eq,PG}$

Table 4. Symbol, Important Model Factors Selected on the Basis of S_i , and Interacting Model Factors Selected on the Basis of S_{Ni} for Each Model Output

Factors	$m_{CO_2,ASP}$			$m_{CO_2,CH_4,comb}$			$m_{CO_2,eq,CH_4,comb}$			$m_{CO_2,eq,CH_4,fugitive}$			$m_{CO_2,eq,CH_4,dewatering}$		
	S_i	S_{Ti}	$S_{Ti} - S_i$	S_i	S_{Ti}	$S_{Ti} - S_i$	S_i	S_{Ti}	$S_{Ti} - S_i$	S_i	S_{Ti}	$S_{Ti} - S_i$	S_i	S_{Ti}	$S_{Ti} - S_i$
μ	0.000	0.001	0.001	0.000	0.003	0.003	0.000	0.003	0.003	0.000	0.003	0.003	0.000	0.000	0.000
k_s	0.000	0.001	0.001	0.000	0.003	0.003	0.000	0.003	0.003	0.000	0.003	0.003	0.000	0.000	0.000
k_d	0.215	0.238	0.023	1.000	0.172	0.024	1.000	0.148	0.172	0.148	0.172	0.024	1.000	0.000	0.000
Y_H	0.000	0.002	0.002	0.066	0.009	0.018	0.009	0.373	0.009	0.018	0.009	0.009	0.373	0.000	0.000
μ_N	0.000	0.002	0.002	0.066	0.003	0.003	0.139	0.003	0.003	0.003	0.003	0.003	0.139	0.000	0.000
K_N	0.000	0.002	0.002	0.066	0.007	0.007	0.290	0.007	0.007	0.007	0.007	0.007	0.290	0.000	0.000
k_{dN}	0.000	0.002	0.002	0.066	0.007	0.007	0.295	0.007	0.007	0.007	0.007	0.007	0.295	0.000	0.000
Y_N	0.000	0.002	0.002	0.066	0.004	0.004	0.157	0.004	0.004	0.004	0.004	0.004	0.157	0.000	0.000
$k_{d,dig}$	0.000	0.002	0.002	0.066	0.004	0.004	0.156	0.004	0.004	0.004	0.004	0.004	0.156	0.000	0.000
$Y_{H,dig}$	0.000	0.002	0.002	0.066	0.005	0.004	0.161	0.005	0.004	0.004	0.004	0.004	0.161	0.000	0.000
pCOD/VSS	0.000	0.002	0.002	0.066	0.150	0.170	0.817	0.150	0.170	0.150	0.170	0.019	0.817	0.000	0.000
nbsCOD _{IN}	0.055	0.057	0.002	0.086	0.004	0.004	0.153	0.004	0.004	0.004	0.004	0.004	0.153	0.000	0.000
pbCOD _{IN}	0.403	0.408	0.005	0.222	0.238	0.017	0.727	0.238	0.017	0.727	0.238	0.017	0.727	0.000	0.000
npbCOD _{IN}	0.300	0.304	0.004	0.189	0.328	0.344	0.671	0.328	0.344	0.671	0.344	0.016	0.671	0.000	0.000
nbsCOD _{Pt}	0.000	0.002	0.002	0.095	0.004	0.004	0.165	0.004	0.004	0.004	0.004	0.004	0.165	0.000	0.000
pbCOD _{Pt}	0.000	0.002	0.002	0.095	0.031	0.036	0.214	0.031	0.036	0.031	0.036	0.005	0.214	0.000	0.000
npbCOD _{Pt}	0.000	0.002	0.002	0.095	0.032	0.038	0.221	0.032	0.038	0.032	0.038	0.005	0.221	0.000	0.000
Q _{dewa}	0.000	0.002	0.002	0.095	0.004	0.004	0.158	0.004	0.004	0.004	0.004	0.004	0.158	0.000	0.000
EF _{N2O}	0.000	0.002	0.002	0.095	0.004	0.004	0.158	0.004	0.004	0.004	0.004	0.004	0.158	0.000	0.000
EF _{CO2}	0.000	0.002	0.002	0.095	0.004	0.004	0.158	0.004	0.004	0.004	0.004	0.004	0.158	0.000	0.000
EF _{CH4}	0.000	0.002	0.002	0.095	0.004	0.004	0.158	0.004	0.004	0.004	0.004	0.004	0.158	0.000	0.000
INVSS _S	0.000	0.002	0.002	0.095	0.004	0.004	0.158	0.004	0.004	0.004	0.004	0.004	0.158	0.000	0.000
INVSS _{S5}	0.000	0.002	0.002	0.095	0.004	0.004	0.158	0.004	0.004	0.004	0.004	0.004	0.158	0.000	0.000
iCOD _{N2Ox}	0.000	0.002	0.002	0.095	0.004	0.004	0.158	0.004	0.004	0.004	0.004	0.004	0.158	0.000	0.000
iCOD _{N2}	0.000	0.002	0.002	0.095	0.004	0.004	0.158	0.004	0.004	0.004	0.004	0.004	0.158	0.000	0.000
CH _{4,SE}	0.000	0.002	0.002	0.095	0.004	0.004	0.158	0.004	0.004	0.004	0.004	0.004	0.158	0.000	0.000
ΣS	0.972	1.048	—	—	0.922	1.093	—	0.922	1.093	—	0.922	1.093	—	0.998	1.001

Factors	$m_{CO_2,eq,N2O,eff}$			$m_{CO_2,eq,PG}$			$m_{CO_2,eq,offset}$			$m_{CO_2,eq,TB}$			η_{CODPS}		
	S_i	S_{Ti}	$S_{Ti} - S_i$	S_i	S_{Ti}	$S_{Ti} - S_i$	S_i	S_{Ti}	$S_{Ti} - S_i$	S_i	S_{Ti}	$S_{Ti} - S_i$	S_i	S_{Ti}	$S_{Ti} - S_i$
μ	0.000	0.000	0.000	0.001	0.098	0.098	0.254	0.003	0.003	0.003	0.003	0.003	0.000	0.001	0.001
k_s	0.000	0.000	0.000	0.009	0.099	0.098	0.254	0.003	0.003	0.003	0.003	0.003	0.000	0.001	0.001
k_d	0.000	0.000	0.000	0.122	0.248	0.126	0.326	0.124	0.144	0.020	1.000	0.023	0.023	0.001	0.001
Y_H	0.000	0.000	0.000	0.056	0.159	0.103	0.268	0.008	0.015	0.007	0.365	0.049	0.054	0.001	0.001
μ_N	0.000	0.000	0.000	0.009	0.011	0.117	0.106	0.275	0.000	0.003	0.003	0.003	0.003	0.001	0.001
K_N	0.000	0.000	0.000	0.009	0.003	0.381	0.981	0.000	0.006	0.006	0.293	0.000	0.004	0.001	0.001
k_{dN}	0.000	0.000	0.000	0.009	0.003	0.388	1.000	0.000	0.006	0.006	0.298	0.000	0.004	0.001	0.001
Y_N	0.000	0.000	0.000	0.009	0.002	0.129	0.329	0.000	0.003	0.003	0.163	0.000	0.003	0.001	0.001
$k_{d,dig}$	0.000	0.000	0.000	0.009	0.002	0.130	0.128	0.333	0.000	0.003	0.161	0.000	0.003	0.001	0.001
$Y_{H,dig}$	0.000	0.000	0.000	0.009	0.002	0.130	0.128	0.333	0.001	0.005	0.168	0.000	0.003	0.001	0.001
pCOD/VSS	0.000	0.000	0.000	0.009	0.007	0.136	0.129	0.335	0.149	0.169	0.955	0.000	0.003	0.001	0.001
nbsCOD _{IN}	0.000	0.000	0.000	0.009	0.044	0.172	0.128	0.333	0.000	0.004	0.180	0.002	0.005	0.001	0.001
pbCOD _{IN}	0.000	0.000	0.000	0.009	0.214	0.344	0.130	0.337	0.220	0.238	0.864	0.612	0.624	0.754	0.002
npbCOD _{IN}	0.000	0.000	0.000	0.009	0.326	0.456	0.130	0.336	0.327	0.344	0.809	0.294	0.306	0.248	0.002
nbsCOD _{Pt}	0.000	0.000	0.000	0.009	0.002	0.130	0.128	0.332	0.000	0.004	0.199	0.000	0.005	0.002	0.002
pbCOD _{Pt}	0.000	0.000	0.000	0.009	0.005	0.132	0.127	0.330	0.031	0.036	0.262	0.001	0.006	0.002	0.002
npbCOD _{Pt}	0.000	0.000	0.000	0.009	0.006	0.132	0.126	0.327	0.032	0.038	0.268	0.001	0.006	0.002	0.002

Table 4. (Continued.)

Factors	$m_{CO_2eq,N_2O,eff}$			$m_{CO_2eq,PG}$			$m_{CO_2eq,offset}$			$m_{CO_2eq,TB}$			η_{CODPS}		
	S_i	S_{Ti}	S_{Ni}	S_i	S_{Ti}	S_{Ni}	S_i	S_{Ti}	S_{Ni}	S_i	S_{Ti}	S_{Ni}	S_i	S_{Ti}	S_{Ni}
Q_{dewa}	0.000	0.000	0.009	0.002	0.128	0.125	0.000	0.004	0.004	0.000	0.005	0.427	0.000	0.002	1.000
EF_{N_2O}	0.998	1.000	1.000	0.002	0.126	0.124	0.000	0.004	0.004	0.000	0.005	0.427	0.000	0.002	1.000
EF_{CO_2}	0.000	0.000	0.016	0.002	0.126	0.124	0.000	0.004	0.004	0.000	0.005	0.427	0.000	0.002	1.000
EF_{CH_4}	0.000	0.000	0.016	0.002	0.126	0.124	0.000	0.004	0.004	0.000	0.005	0.427	0.000	0.002	1.000
$INVSS_{PS}$	0.000	0.000	0.016	0.002	0.126	0.124	0.000	0.004	0.004	0.000	0.005	0.427	0.000	0.002	1.000
$INVSS_{SS}$	0.000	0.000	0.016	0.002	0.126	0.124	0.000	0.004	0.004	0.000	0.005	0.427	0.000	0.002	1.000
$iCOD_{NOx}$	0.000	0.000	0.016	0.031	0.169	0.138	0.359	0.004	0.004	0.000	0.005	0.427	0.000	0.002	1.000
$iCOD_{N_2}$	0.000	0.000	0.016	0.015	0.234	0.219	0.569	0.004	0.004	0.000	0.005	0.427	0.000	0.002	1.000
$CH_{4,SE}$	0.000	0.000	0.016	0.003	0.222	0.219	0.568	0.032	0.039	0.007	0.005	0.427	0.000	0.002	1.000
ΣS	0.998	1.001	—	0.869	4.761	—	—	0.925	1.095	—	1.107	—	0.998	1.043	—

Note: Important model factors are in bold.

thus influencing the $m_{CO_2eq,PG}$ of the aeration process and of the entire WWTP.

The influence of the conversion factors $iCOD_{NOx}$ and $iCOD_{N_2}$ is mainly related to the variation of the oxygen requirement on the basis of the COD availability for heterotrophic biomass growth at low dissolved oxygen concentration. Furthermore, the influence of μ_N in terms of S_i is related to the oxygen requirement for autotrophic biomass growth.

High interaction among factors has been found for the $m_{CO_2eq,PG}$ model output (Table 4), as confirmed by the high value of the ΣS_{Ti} (4.761). The high interaction is mainly due to the complexity of the model in terms of $m_{CO_2eq,PG}$. The total $m_{CO_2eq,PG}$ are computed by summing the single processes' power requirements. Among the interacting factors, those having the highest contribution to the total model variance are k_N and k_{dN} . These two model factors are related to the kinetics of the autotrophic biomass. In fact, autotrophic biomass growth influences the aeration requirement inside the aerobic tank.

As discussed previously, the slight difference between the results of SRC and Extended-FAST application for the four model outputs taken into account are a result of the selection of the important and noninfluential model factors (Fig. 3). Indeed, for each GSA method applied, model factors that were important (and interacting for the Extended-FAST application) for at least one model output have been considered important for the entire model; all the other factors have been considered noninfluential. An analysis of Fig. 3(a) shows that the Extended-FAST method overestimates the number of important factors due to the inclusion of the interacting factors that cannot be selected by means of the SRC method. Indeed, while 20 model factors have been classified as important for the Extended-FAST application, only 14 model factors have the same classification for SRC. Consequently, the SRC application provides a higher number (12) of noninfluential model factors than the Extended-FAST (6) [Fig. 3(b)]. Specifically, the role of nitrogen removal processes in producing GHGs is emphasized by applying the Extended-FAST method with the inclusion of the importance of factors μ_N , k_d , k_{dN} , $INVSS_{PS}$, and $INVSS_{SS}$. Indeed, these factors can directly (μ_N , k_d , and k_{dN}) or indirectly ($INVSS_{PS}$ and $INVSS_{SS}$) regulate the activity of the autotrophic biomass. Thus, results obtained by using the Extended-FAST method suggest that the modeler should be attentive to the processes that involve autotrophic biomass in view to control the GHG production at plantwide scale.

The important model factors reported in the Venn diagram have been classified on the basis of β_i (for SRC) and S_i and S_{Ni} (for Extended-FAST).

Uncertainty Analysis

The uncertainty analysis was performed by fixing the noninfluential factors at their default values (Table 1) and considering only the model factors that are important for at least one model output. The uncertainty analysis was conducted twice, first using the results of the SRC application, and then the results of the Extended-FAST. Each time the same number of simulations carried out for the GSA method application has been performed.

The comparison of the uncertainty analysis results among the model outputs has been performed by means of the relative uncertainty bands width values. These latter were evaluated dividing the bandwidth—calculated as the difference between the 5th and 95th percentile—of the perturbed output distribution, by the 50th percentile.

Fig. 4 shows the CDFs, obtained by running simulations using the results of SRC and Extended-FAST applications for $m_{CO_2,ASP}$,

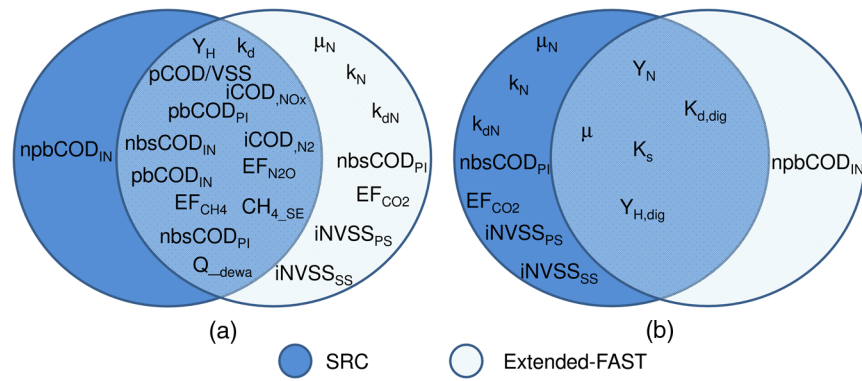


Fig. 3. Venn diagram related to the comparison of (a) important and (b) noninfluential factors obtained by applying SRC and Extended-FAST

$m_{CO2eq,CH4,comb}$, $m_{CO2eq,CH4,dewatering}$, and $m_{CO2eq,PG}$. The 5th and 95th percentiles of each CDF have been also calculated.

A visual inspection of Fig. 4 reveals that the uncertainty bandwidth values change with the model output and with the results of GSA applications used for the analysis. The difference among model outputs is mainly due to the fact that some of the model outputs entail a different level of complexity in terms of involved phenomena. The difference between the two uncertainty analysis applications (using the results of SRC and Extended-FAST) is mainly due to the different set of factors involved during the analysis.

Specifically, the uncertainty bandwidth of $m_{CO2,ASP}$ (605 and 567 $g\ CO_2\ m^{-3}$ by using SRC and Extended-FAST results, respectively) and $m_{CO2eq,CH4,comb}$ (498 and 513 $g\ CO_{2eq}\ m^{-3}$ by using SRC and Extended-FAST results, respectively) are higher than $m_{CO2eq,CH4,dewatering}$ (4.4 and 4.2 $g\ CO_{2eq}\ m^{-3}$ by using SRC and Extended-FAST results, respectively) and $m_{CO2eq,PG}$ (179 and 164 $g\ CO_{2eq}\ m^{-3}$ by using SRC and Extended-FAST results, respectively). In general, results obtained after applying SRC provide a higher uncertainty bandwidth for the model outputs $m_{CO2,ASP}$, $m_{CO2eq,CH4,dewatering}$, and $m_{CO2eq,PG}$. Thus, except for $m_{CO2eq,CH4,comb}$, including the effect of the interacting factors (with the Extended-FAST application) the model uncertainty decreases. For example, including the model factors μ_N , k_d , k_{dN} , $iNVSS_{PS}$,

and $iNVSS_{SS}$ selected as interacting by means of the Extended-FAST method, the modeler can optimize the contribution of the GHG production due to the autotrophic activity. However, the inclusion of these model factors can have a negative influence on $m_{CO2eq,CH4,comb}$ uncertainty due to the different autotrophic biomass activity a different carbon to nitrogen (C/N) ratio of the secondary sludge causes, thus influencing the quality of the biogas produced.

The uncertainty analysis based only on the width of the uncertainty band can be misleading because this width is influenced by the order of magnitude of the considered model output.

Thus, in order to provide a quantitative assessment of the model uncertainty and to make the results comparable among the model outputs, the relative uncertainty bandwidth for each model output has been computed.

Fig. 5 shows the relative uncertainty bandwidth for each model output and for each uncertainty analysis application. An analysis of Fig. 5 shows that the highest uncertainty for both applications is related to the $m_{CO2eq,N2O,eff}$ (the relative uncertainty bandwidth is equal to 1.63). This fact may be due to the value of the EF_{N2O} used to quantify N_2O emitted with the effluent.

EF is based on the Intergovernmental Panel on Climate Change (IPCC) (2006) recommendation. However, as reported in literature, the EFs suggested by the IPCC are highly uncertain due to the wide range of measured values used for EF definition

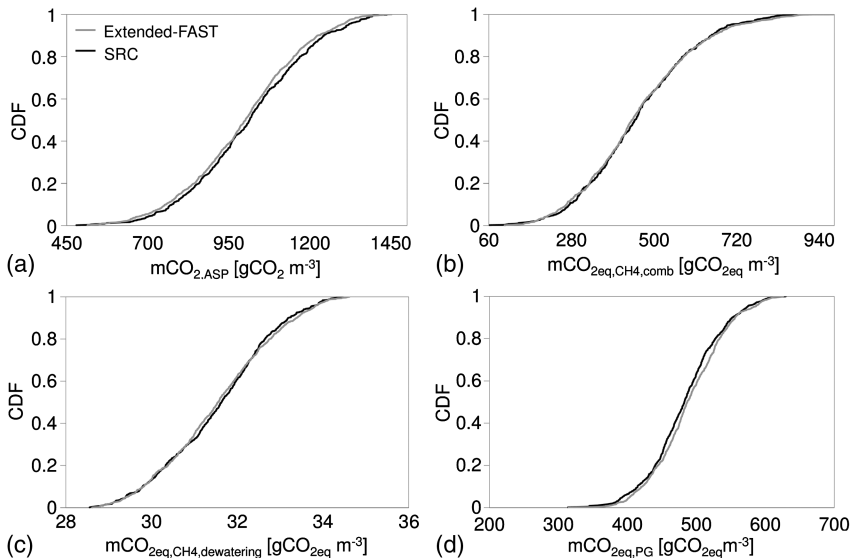


Fig. 4. CDF of (a) $m_{CO2,ASP}$; (b) $m_{CO2eq,CH4,comb}$; (c) $m_{CO2eq,CH4,dewatering}$; (d) $m_{CO2eq,PG}$

Downloaded from ascelibrary.org by Giorgio Mammia on 06/16/16. Copyright ASCE. For personal use only; all rights reserved.

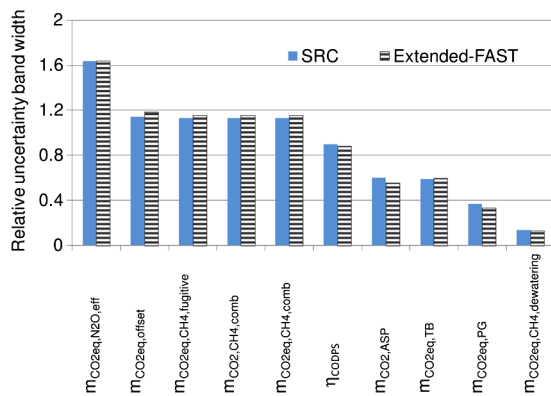


Fig. 5. Relative uncertainty bandwidth for each model output

(Flores-Alsina et al. 2014). Within this context, the N_2O emission quantification could be improved by including the processes occurring in the receiving water body. In fact, if bCOD or nutrients are not removed inside a process they undergo inexorable (albeit slow) biodegradation in the receiving environment, which is the carbon footprint of no treatment (Rosso and Stenstrom 2008).

Fig. 5 also reveals that a high and comparable uncertainty degree was found for $m_{CO_2,CH_4,comb}$, $m_{CO_2eq,CH_4,comb}$, $m_{CO_2eq,CH_4,fugitive}$, and $m_{CO_2eq,offset}$ (the relative uncertainty bandwidth is approximately 1.12 and 1.15 using the SRC and Extended-FAST results, respectively). The high uncertainty for these latter model outputs can be attributed to the complexity of the processes and consequently of the algorithms that describe their dynamics. These algorithms involve several model factors such as the influent COD fractionation, pCOD/VSS, and COD fractionation factors related to the primary effluent. Future studies, based on measured data, should be performed in order to clearly split the role of the uncertainty of each factor involved in the $m_{CO_2,CH_4,comb}$, $m_{CO_2eq,CH_4,comb}$, $m_{CO_2eq,CH_4,fugitive}$, and $m_{CO_2eq,offset}$ model outputs.

In order to provide an overall effect of each process in terms of total equivalent CO_2 production, Fig. 6 reports the percentage production related to the processes taken into account.

As shown in Fig. 6, the two greatest CO_2 emissions are related to the total biosolids discharge (40.24%) and to the biomass respiration (30.45%). This result suggests optimizing the biological processes in order to reduce the percentage of the total CO_2 emitted.

Conclusions

Sensitivity analysis methods have revealed that model factors characterizing influent and primary wastewater in terms of COD (e.g., $nbsCOD_{IN}$ and $pbCOD_{IN}$) have a significant impact in modeling GHGs. The role of factor pCOD/VSS was found to be relevant especially in terms of factor interaction. Model factors related to the autotrophic biomass growth were found to strongly influence the total model variance in terms of interaction, especially regarding the indirect GHG emission. Model factors selected as influential or interacting should be better quantified (e.g., by means of ad hoc laboratory tests) in order to improve model predictions.

The uncertainty analysis shows that $m_{CO_2eq,N_2O,eff}$ has the highest uncertainty in terms of relative uncertainty band (1.63). This result suggests that EF adopted for the N_2O effluent quantification should be improved to provide accurate results.

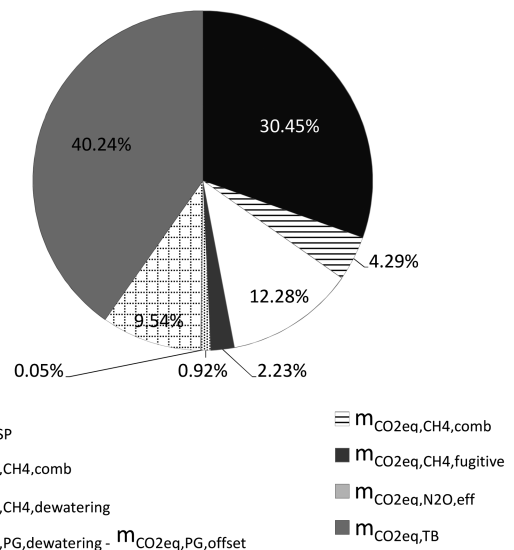


Fig. 6. Percentage of CO_2 emission related to the following processes: biomass respiration ($m_{CO_2,ASP}$), biogas combustion ($m_{CO_2,CH_4,comb}$, $m_{CO_2eq,CH_4,comb}$), fugitive emissions ($m_{CO_2eq,CH_4,fugitive}$), dewatering ($m_{CO_2eq,CH_4,dewatering}$), effluent discharge ($m_{CO_2eq,N_2O,eff}$), net power requirements ($m_{CO_2eq,PG} - m_{CO_2eq,offset}$), and biosolids discharge ($m_{CO_2eq,TB}$)

The derived results have to be interpreted in the context that has been herein formulated—thus not having a universal validity. Despite such a limit, the results demonstrate the paramount importance in the evaluation of sensitivity and uncertainty analysis in order to get robust results by identifying the key uncertainty sources and designing ad hoc laboratory test.

Acknowledgments

This work forms a part of a research project supported by grant of the Italian Ministry of Education, University and Research (MIUR) through the Research Project of National Interest PRIN2012 (D.M. 28 dicembre 2012 n. 957/Ric—Prot. 2012PTZAMC) entitled “Energy consumption and greenhouse gas (GHG) emissions in the wastewater treatment plants: A decision support system for planning and management” in which the corresponding author is the principal investigator (<http://ghgfromwwtp.unipa.it>).

References

- Ahn, J. H., Kim, S., Park, H., Rahm, B., Pagilla, K., and Chandran, K. (2010). “ N_2O emissions from activated sludge processes, 2008–2009: Results of a national monitoring survey in the United States.” *Environ. Sci. Technol.*, 44(12), 4505–4511.
- Brun, R., Kühni, M., Siegrist, H., Gujer, W., and Reichert, P. (2002). “Practical identifiability of ASM2d parameters: Systematic selection and tuning of parameter subsets.” *Water Res.*, 36(16), 4113–4127.
- Cakir, F. Y., and Stenstrom, M. K. (2005). “Greenhouse gas production: A comparison between aerobic and anaerobic wastewater treatment technology.” *Water Res.*, 39(17), 4197–4203.
- Caniani, D., Esposito, G., Gori, R., and Mannina, G. (2015). “Towards a new decision support system for design, management and operation of wastewater treatment plants for the reduction of greenhouse gases emission.” *Water*, 7(10), 5599–5616.
- Corominas, L., Flores-Alsina, X., Snip, L., and Vanrolleghem, P. A. (2012). “Comparison of different modeling approaches to better

- evaluate greenhouse gas emissions from whole wastewater treatment plants." *Biotechnol. Bioeng.*, 109(11), 2854–2863.
- Cosenza, A., Mannina, G., Neumann, M. B., Viviani, G., and Vanrolleghem, P. A. (2013a). "Biological nitrogen and phosphorus removal in membrane bioreactors: Model development and parameter estimation." *Bioproc. Biosyst. Eng.*, 36(4), 499–514.
- Cosenza, A., Mannina, G., Vanrolleghem, P. A., and Neumann, M. B. (2013b). "Global sensitivity analysis in wastewater applications: A comprehensive comparison of different methods." *Environ. Modell. Software*, 49, 40–52.
- Czepiel, P., Crill, P., and Harriss, R. (1995). "Nitrous-oxide emissions from municipal waste-water treatment." *Environ. Sci. Technol.*, 29(9), 2352–2356.
- Czepiel, P., Crill, P. C., and Harriss, R. C. (1993). "Methane emissions from municipal wastewater treatment processes." *Environ. Sci. Technol.*, 27(12), 2472–2477.
- Daelman, M. R. J., van Voorthuizen, E. M., van Dongen, U. G. J. M., Volcke, E. I. P., and van Loosdrecht, M. C. M. (2012). "Methane emission during municipal wastewater treatment." *Water Res.*, 46(11), 3657–3670.
- Flores-Alsina, X., et al. (2014). "Balancing effluent quality, economic cost and greenhouse gas emissions during the evaluation of (plant-wide) control/operational strategies in WWTPs." *Sci. Total Environ.*, 466–467, 616–624.
- Flores-Alsina, X., Corominas, L., Snip, L., and Vanrolleghem, P. A. (2011). "Including greenhouse gas emissions during benchmarking of wastewater treatment plant control strategies." *Water Res.*, 45(16), 4700–4710.
- Foley, J., de Haas, D., Yuan, Z., and Lant, P. (2010). "Nitrous oxide generation in full-scale biological nutrient removal wastewater treatment plants." *Water Res.*, 44(3), 831–844.
- Freni, G., and Mannina, G. (2010). "Bayesian approach for uncertainty quantification in water quality modelling: The influence of prior distribution." *J. Hydrol.*, 392(1–2), 31–39.
- Gori, R., Giaccherini, F., Jiang, L.-M., Sobhani, R., and Rosso, D. (2013). "Role of primary sedimentation on plant-wide energy recovery and carbon footprint." *Water Sci. Technol.*, 68(4), 870–878.
- Gori, R., Jiang, L.-M., Sobhani, R., and Rosso, D. (2011). "Effects of soluble and particulate substrate on the carbon and energy footprint of wastewater treatment processes." *Water Res.*, 45(18), 5858–5872.
- GRP (General Reporting Protocol). (2008). "Accurate, transparent, and consistent measurement of greenhouse gases across North America version 1.1." Mountain View, CA.
- GWRC (Global Water Research Coalition). (2011). "N₂O and CH₄ emission from wastewater collection and treatment systems—State of the science report." London.
- Hauduc, H., et al. (2011). "Activated sludge modelling: Development and potential use of a practical applications database." *Water Sci. Technol.*, 63(10), 2164–2182.
- Hiatt, W. C., and Grady, C. P. L., Jr. (2008). "An updated process model for carbon oxidation, nitrification, and denitrification." *Water Environ. Res.*, 80(11), 2145–2156.
- IPCC (Intergovernmental Panel on Climate Change). (2006). "Guidelines for national greenhouse gas inventories." (<http://www.ipcc-nggip.iges.or.jp/public/2006gl/>).
- Kampschreur, M. J., Temmink, H., Kleerebezem, R., Jettena, M. S. M., and van Loosdrecht, M. C. M. (2009). "Nitrous oxide emission during wastewater treatment." *Water Res.*, 43(17), 4093–4103.
- Law, Y., Jacobsen, G., Smith, A., Yuan, Z., Lant, P. (2013). "Fossil organic carbon in wastewater and its fate in treatment plants." *Water Res.*, 47(14), 5270–5281.
- Law, Y., Ye, L., Pan, Y., and Yuan, Z. (2012). "Nitrous oxide emissions from wastewater treatment processes." *Philos. Trans. R. Soc. B.*, 367(1593), 1265–1277.
- LGO (Local Government Operations). (2008). "Local government operations protocol for the quantification and reporting of greenhouse gas emissions inventories, version 1.0." (<http://www.theclimateregistry.org/resources/protocols/local-government-operations-protocol/>) (Sep. 2008).
- Mannina, G., and Cosenza, A. (2015). "Quantifying sensitivity and uncertainty analysis of a new mathematical model for the evaluation of greenhouse gas emissions from membrane bioreactors." *J. Membr. Sci.*, 475(1), 80–90.
- Mannina, G., Cosenza, A., Randrianantoandro, M., Anctil, F., Neumann, M. B., and Vanrolleghem, P. A. (2014). "Global sensitivity analysis in environmental water quality modelling: Where do we stand?" *Proc., 7th Int. Congress on Environmental Modelling and Software: Bold Visions for Environmental Modeling*, iEMSs, San Diego, 619.
- Mannina, G., Cosenza, A., Vanrolleghem, P. A., and Viviani, G. (2011). "A practical protocol for calibration of nutrient removal wastewater treatment models." *J. Hydroinf.*, 13(4), 575–595.
- Monteith, H. D., Sahely, H. R., MacLean, H. L., and Bagley, D. M. (2005). "A rational procedure for estimation of greenhouse-gas emissions from municipal wastewater treatment plants." *Water Environ. Res.*, 77(4), 390–403.
- Neumann, M. B. (2012). "Comparison of sensitivity analysis techniques for modelling micropollutant oxidation in water treatment." *Sci. Total Environ.*, 433(1), 530–537.
- Ni, B. J., Ruscalleda, M., Pellicer-Nacher, C., and Smets, B. F. (2011). "Modeling nitrous oxide production during biological nitrogen removal via nitrification and denitrification: Extensions to the general ASM models." *Environ. Sci. Technol.*, 45(18), 7768–7776.
- Ni, B. J., Ye, L., Law, Y., Byers, C., and Yuan, Z. (2013a). "Mathematical modeling of nitrous oxide (N₂O) emissions from full-scale wastewater treatment plants." *Environ. Sci. Technol.*, 47(14), 7795–7803.
- Ni, B. J., Yuan, Z., Chandran, K., Vanrolleghem, P. A., and Murthy, S. (2013b). "Evaluating four mathematical models for nitrous oxide production by autotrophic ammonia-oxidizing bacteria." *Biotechnol. Bioeng.*, 110(1), 153–163.
- Pagilla, K., Shaw, A., Kunetz, T., and Schiltz, M. (2009). "A systematic approach to establishing carbon footprints for wastewater treatment plants." *Proc. Water Environ. Fed.*, 2009(10), 5399–5409.
- Pujol, G. (2007). "Sensitivity: Sensitivity analysis, R package version 1.3–0." R Development Core Team, France.
- Rosso, D., and Stenstrom, M. K. (2008). "The carbon-sequestration potential of municipal wastewater treatment." *Chemosphere*, 70(8), 1468–1475.
- Saltelli, A., et al. (2008). *Global sensitivity analysis, the primer*, Wiley, Chichester, U.K.
- Sin, G., Gernaey, K. V., Neumann, M. B., van Loosdrecht, M., and Gujer, W. (2011). "Global sensitivity analysis in wastewater treatment plant model applications: Prioritizing sources of uncertainty." *Water Res.*, 45(2), 639–651.
- Sweetapple, C., Fu, G., and Butler, D. (2013). "Identifying key sources of uncertainty in the modelling of greenhouse gas emissions from wastewater treatment." *Water Res.*, 47(13), 4652–4665.
- Townsend-Small, A., Pataki, D. E., Tseng, L. Y., Tsai, C.-Y., and Rosso, D. (2011). "Nitrous oxide emissions from wastewater treatment and water reclamation plants in southern California." *J. Environ. Qual.*, 40(5), 1542–1550.
- Vanrolleghem, P. A., Mannina, G., Cosenza, A., and Neumann, M. B. (2015). "Global sensitivity analysis for urban water quality modelling: Terminology, convergence and comparison of different methods." *J. Hydrol.*, 522, 339–352.
- WEF (Water Environment Federation). (2009). *Energy conservation in water and wastewater facilities—MOP 32*, Alexandria, VA.
- Weijers, S. R., and Vanrolleghem, P. A. (1997). "A procedure for selecting best identifiable parameters in calibrating activated sludge model no. 1 to full-scale plant data." *Water Sci. Technol.*, 36(5), 69–79.